AJEMA GLOBAL RESEARCH NETWORK

AMERICAN Journal of Engineering, Mechanics and Architecture
Volume 3, Issue 11, 2025 ISSN (E): 2993-2637

Innovative Integration of Hybrid Energy Sources for Air Conditioning and Space Heating Systems: Maximizing Performance with Solar Energy and Advanced Evacuated Collector Technologies

Yahea A. Nasser
Chemical Department, Engineering College, Al Muthanna University, Muthanna, Iraq

Abstract: The hybrid design of Cooling and air-conditioning establishes the main consumers of building energy in areas branded by hot and cold climatic circumstances. The examined design includes six unit components: compressor, shell-and-tube heat exchanger, expansion valve, a coil-and-tank, a vacuum collector, and a solar power. Several experiments were conducted by methodically changing important working limits to measure their effect on the thermal presentation of the hybrid design system. The inspected limits comprised cooling discharge (2, 3, 4, and 5 L/min), temperature (14, 12, 10, and 8 °C), refrigerant mass rate (70, 50, and 30 kg/h), tank temperature (80, 75, and 70 °C), and solar light intensity under the meteorological conditions of Muthanna in Iraqi. The results exposed that the design's presentation declines with an increase in temperature from 8 °C to 14 °C, the coefficient of performance (COP) lower from 2.8 to 1.98, accompanied by an increase in consumption of compressor power from 650 W to 980 W. Also, the thermal performance of the design was found to be markedly affected by the cooling water discharge. An improvement in discharge led to a consistent development in the COP. When the cooling discharge increased from 2 L/min to 6 L/min, the COP improved from 2.6 to 3.2, though consumption of compressor power reduced from 1050 W to 670 W.

Keywords: power energy, renewable energy systems, thermal collectors, solar energy, evacuated solar collector.

1. Introduction

construction signifies one of the main power-consuming sectors internationally, needful considerable quantities of energy for its process. Together, buildings explanation for about 40% of the world's total yearly energy consumption, chiefly for illumination, heating, cooling, and air-conditioning. In the new year, the ideas of maintainable systems and building have gained substantial fame within the building manufacturing[1] . Engineers progressively know that through brainy system plans, it is likely to meaningfully reduce power consumption and alleviate the ecological footprint of structures [2] .Sustainably designed structures that assimilate renewable energy schemes strive to function with negligible need for non-renewable energy sources [3]. This method efficiently decreases ecological influences throughout the structure development. It is projected that about 1.74×10^{17} watts of solar energy strikes the Earth's outer sky, around 30% is copied back into space, though the remaining 70% is absorbed by the Earth's oceans, land surfaces, and impressive mechanisms [4]. So, the total solar power engrossed by the atmosphere, oceans, and landmass is about 3.85×10^{24} (j/yr), with 2.8×10^{24} J engrossed by terrestrial and sea schemes .According to BP's global energy report [5] , total universal power consumption in 2008 was assessed at 4.74×10^{20} J, with more than 80% resulting from fossil

fuel combustion. This comparison designates that the solar power absorbed yearly by the land and sea is 5900 times greater than the total global power consumption in 2007. In detail, the solar energy engrossed by the Ground in just one hour generates the total quantity of energy expended globally within a complete year, underlining the huge potential of solar power as a clean, sustainable alternative to fossil fuels[6].Rising ecological anxieties, attached with incessant progressions in study and technical novelty, have considerably increased global interest in solar-assisted air-conditioning (SAC) designs. Many protest projects worldwide have long-established the technical adulthood and working dependability of SAC designs [7]. Though no pilot-scale applications of such designs have been led in Iraq to date. Associated with traditional air-conditioning processes, solar-assisted designs offer multiple compensations solar-assisted air [8]. They decrease dependence on grid electricity, lower working costs, and minimize greenhouse gas emissions. Besides, SAC designs exhibit peak presentation during the summer period—exactly when cooling demands are uppermost—thus contributing to the discount of electrical peak loads related to conventional grid-dependent cooling designs [9].Widespread assignment of SAC systems has the conceivable to meaningfully reduce grid-based electricity consumption and, concurrently, decrease capital spending associated with power generation and distribution infrastructure. Thermally driven solar air-conditioning skills offer an extra advantage: in areas where cooling is obligatory seasonally, the same designs can be applied for domestic hot water production or other thermal requests [10]. Though the intermittent nature of solar radiation has limited customer adoption, such disadvantages can be alleviated through the addition of supplementary designs powered by conservative fuels or through thermal inclusion [11] .So, the design of the hybrid design must be prudently enhanced to achieve user supplies while exploiting power competence and ecological aids [12]. In spite of the many compensations of SAC designs over conservative air-conditioning systems, numerous mechanical, financial, and policy-associated barriers last to obstruct their large-scale placement[13]. Though solutions to practical tests are being industrialized, the financial viability and supportive policy frameworks continue to be vital for enabling marketplace expansion [14]. A thorough review of the global marketplace route reveals important potential for the large-scale acceptance of SAC skills, eased by improved design competence, increased public consciousness, and promising governmental rules [15]. The rising interest in solar-based cooling requests has made a wide body of literature encompassing experimental presentation analyses, design demonstrations, and real-world case studies of successful application [16].Amongst the numerous system configurations, combined solar air-conditioning designs have gained specific attention because of their ecological compensations and reduced power consumption compared to conservative designs [17]. These combined designs utilize solar thermal energy as a supplementary heat source to support the vapor compression refrigeration procedure, thus lessening the overall electrical power demand [18].The present work aims to examine the effect of key working limits—for instance, room temperature, solar energy intensity, and cooling load—on the COP, cooling capacity, and energy consumption of a vapor compression refrigeration design. The work includes the systems and building of a solar-assisted vapor compression refrigeration new setup, shadowed by a complete assessment of its thermal performance.

2. Experimental

2.1 Instrumentation and Measurements

The equipment was outfitted with the required instrumentation to assess the prototype's performance in several scenarios. A schematic diagram of the device that shows where the instrumentation is located within the prototype. Variations in the temperature and flow rate of cooling water, heating water, refrigerant, electrical voltage and power, ambient temperature, and solar intensity were all detected by a variety of monitoring equipment.

2.2 Solar Radiation Intensity

The Ministry of Industry and Minerals' department of research and industrial development provided the ambient temperature and solar intensity data for Al Muthanna City, which is two to three kilometers distant from the collector.

2.3 The solar system design

The solar system design contains the evaporator, collector loop, and compressor. The evaporator is made up of a 2 m, 5/8-inch-diameter copper coil flooded in a 25-liter water tank that is 25 cm in diameter and 35 cm in height. The piping diagram of the prototype design, which comprises all of the system's installed arrangement, is shown in Figure 1, where each of the three loops has a clear label with R-24 as the working fluid, the air conditioning loop is associated in series with the cooling tower loop, and the charge loop. The evaporator bent into a spiral coil, filling the whole height of the galvanized steel tank to maximize heat exchange. A ball valve is installed as a safety device to prevent the tank from overflowing. The tank is insulated to reduce heat loss to the environment, preserving the temperature of the water for use. In a typical solar heating system, the collector loop transfers heat from the solar collectors to the balance of the system. The experimental solar heating loop is composed of an evacuated tube solar collector, a circulating water pump, and a heat exchanger. In the present study, the evacuated tube solar collector comprises fourteen (14) borosilicate glass tubes, each with a total length of 180 cm, supplying heated water to a horizontal storage tank with a capacity of 50 liters. The circulation of water within the collector operates through natural convection, wherein the heated water ascends through the tubes and is continuously replaced by cooler water from below. The hot water generated accumulates in the storage tank, ensuring a continuous supply for the system.

The collector assembly is mounted on a steel support structure that allows for flexible adjustment of the tilt and azimuth angles (β, γ) to accommodate various geographic locations. For standard operation, the collector tilt angle (β) is set to 45° from the horizontal, while the azimuth angle (γ) is set to 0°, corresponding to a south-facing orientation suitable for sites located in the Northern Hemisphere.Each evacuated tube consists of two concentric borosilicate glass cylinders fused at the top and hermetically sealed at the bottom to create a vacuum layer between them. The outer glass tube has an external diameter of 4.8 cm and a length of 150 cm, while the inner (absorber) tube has an internal diameter of 3.6 cm and an effective length of approximately 150 cm, accounting for a 6 cm deduction corresponding to the tank wall thickness. Each tube holds approximately 2.5 liters of water, and both the inner and outer walls have a thickness of 0.14 cm.The inner tube, which contains the working fluid (water), is externally coated with a dark nitrite aluminum layer characterized by high absorptivity and thermal conductivity. This selective coating enhances the absorption of incident solar radiation and facilitates efficient heat transfer to the water inside. The evacuated annular space between the two glass walls functions as an effective thermal insulator, minimizing heat losses by suppressing both convective and conductive mechanisms. Consequently, the absorbed solar energy is retained within the system, reducing radiative losses to the surroundings through the greenhouse effect.The entire evacuated tube assembly is supported at its lower edge by a horizontal spring-mounted holder containing a barium getter, which maintains the vacuum integrity within the tubes and ensures long-term thermal performance stability.

The water in the basin at the bottom of the tower was kept at (120 mm) level height constant using a system of a controlling float valve connected to the make–up water tank (upper tank) of (400 mm) diameter and (850 mm) height.The tower basin also has a drain pipe (44 mm) diameter to drain the overflow water to the drain tank (lower tank) of (400 mm) diameter and (850 mm) height.A 2.54 cm copper tube having nine nozzles was used to distribute the water over the water distributor basin, which was made of a (2 mm) thick Perspex colorless plate with (15 × 6) number of holes. These holes are of (1.5 mm) diameter, designed in such a way that the drops of water are evenly dispersed over the packing.

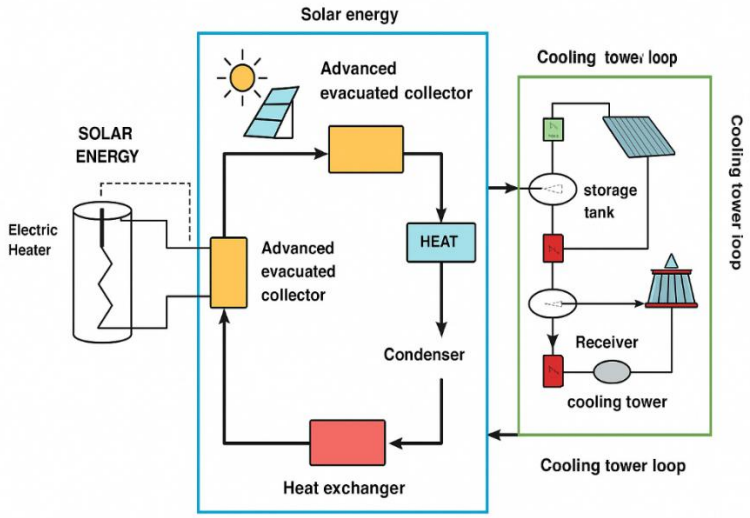

Figure 1: The diagram of the hybrid design

3. Results and discussion

3.1 The heat transfer rate

The heat transfer rates through both the evaporator and the condenser were calculated. The heat transferred through the evaporator and the condenser was also measured by the energy gained by the refrigerant [19]. Heat transfer through both the evaporator and condenser was calculated, and is shown in Equations (1) and (2):

$$Q_c = \dot{m}_r\ (h_i - h_o\ )\ (1)$$

$$Q_e = \dot{m}_r\ (h_o - h_i\ )\ (2)$$

Where $\dot{m}_r$ is the mass flow rate of the refrigerant, and $h_i$through h_o Signify the enthalpies at the consistent points through the air conditioning loop [20].

3.2 The calculation of COP

When examining the air conditioning system, one of the most crucial factors is the system's COP. It explains how much heat is extracted from cooled water relative to the compressor's real power usage[21]. Equation (3) below displays the formula used to get the air conditioner's COP :

$$\mathrm{COP} = \frac{\mathrm{Q_e}}{\mathrm{W_{comp}}}\ (3)$$

Where Q_e and W_{comp}It is envisioned based on the power increased by the refrigerant and the real electrical power consumption of the compressor, respectively [22].

To find out how well the system worked under different circumstances, a variety of experiments were run. Two types of tests were run: constant flow rate of water in the cooling tower, and constant evaporator water load temperature tests [23]. Different storage tank temperatures and refrigeration flow rates were used for the two types. The cooling tower's constant water flow rate, which corresponds to the condenser tests' constant water flow rate, was operated at 3 liters per minute [24].

and at five different load temperatures (14, 12, 10, 9, and 8 ºC). The constant load temperature tests, which also mean constant water temperature in the evaporator tank, were also run at 12 ºC, and at four different water flow rates in the cooling tower (2.5 l/min, 3.5 l/min, 4.5 l/min, and 6 l/min) [20].

3.3 The Effect of Evaporator Water Temperature

The effect of evaporator water temperature variation on the evaporator and condenser heat transfer rates. These tests were run at a constant water condenser flow rate, $\dot{m}_r$ = (70, 50, and 30)

kg/hr and storage tank water temperatures = (80, 75, and 70) ºC. The influence of evaporator water temperature (load temperature) on the evaporator cooling capacity is presented in Figures 2, 3, and 4 [25]. The information obviously designates that the all-out cooling capacity is reached at a temperature of 14 °C. As the load temperature increases, the consistent temperature also increases, subsequent in a notable improvement in cooling capacity—from an average of about 1700 W to 2800 W. This development can be credited to the higher enthalpy change and the augmented inlet vapor density under elevated temperature circumstances [26]. Figures 5–7 further prove that the condenser heat transfer rate of the air-conditioning system exhibits a relative upsurge with the evaporating temperature. This conduct rises from the enhanced evaporator heat transfer rate, which elevates the refrigerant temperature at the condenser input. So, the enthalpy change across the condenser upsurges, thus supplementing the overall condenser heat transfer rate. As the evaporating temperature upsurges from 8 °C to 14 °C, the condenser heat transfer rate consistently rises from an average of 2100 W to 3700 W[27]. Conversely, at lower temperatures, a deterioration in cooling capacity is experiential—commonly. Under these circumstances, inadequate refrigerant flow limits the heat absorption within the evaporator, lessening the local heat transfer coefficient and, so, plummeting the overall cooling performance of the scheme [28].

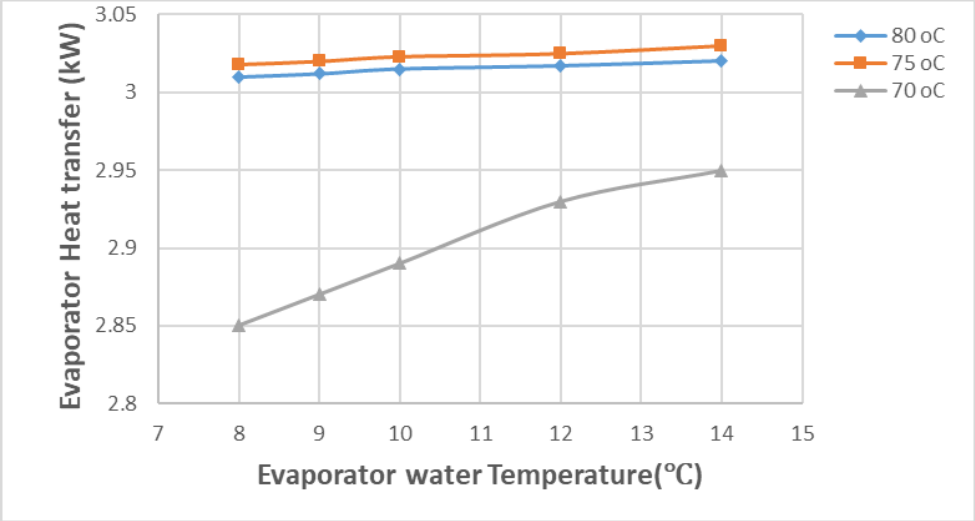

Figure 2: change of heat transfer rates with water temperature at 70 kg/hr

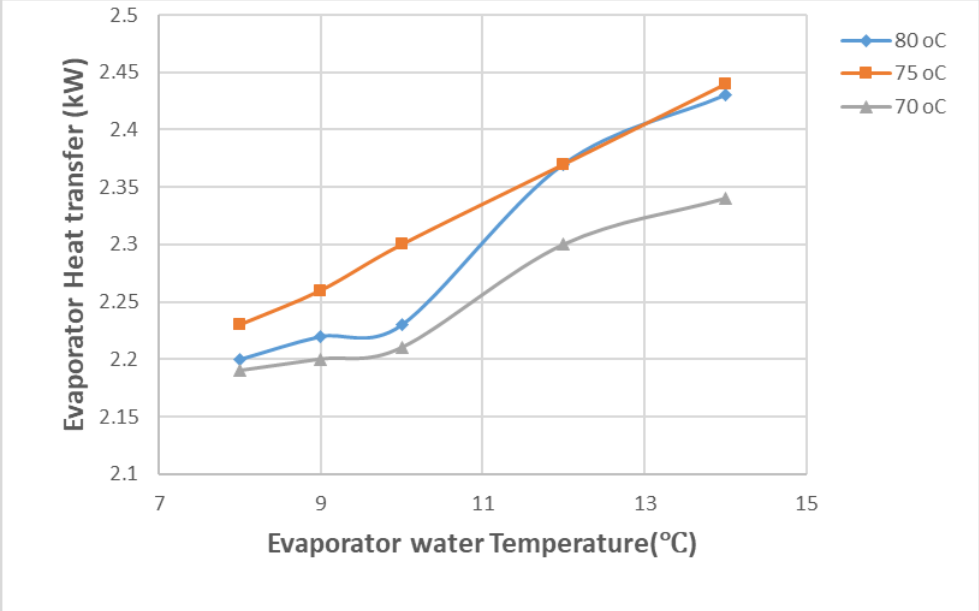

Figure 3: change of heat transfer rates with water temperature at 50 kg/hr

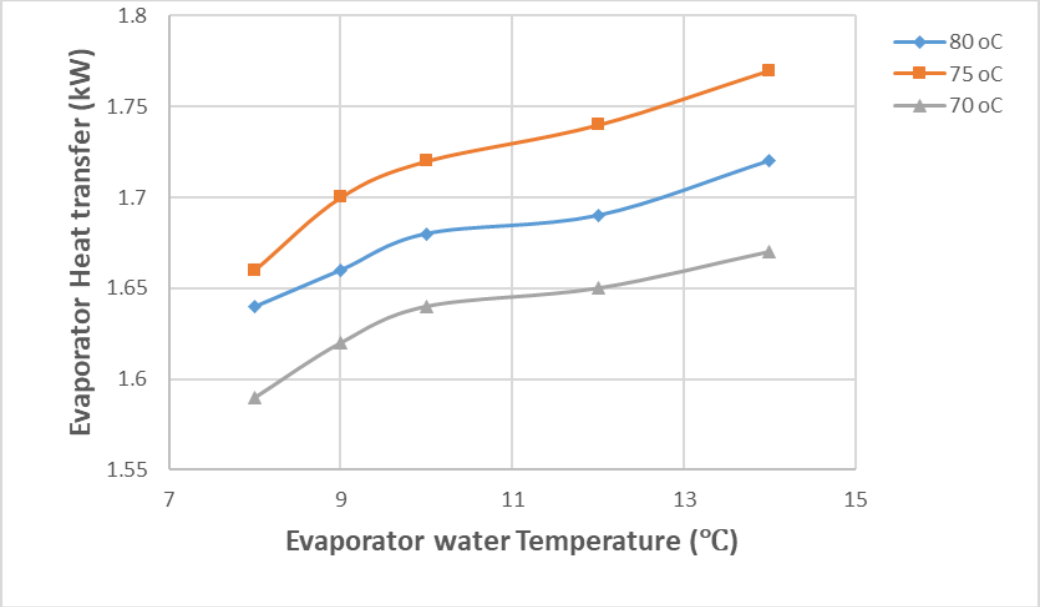

Figure 4: change of heat transfer rates with water temperature at 30 kg/hr

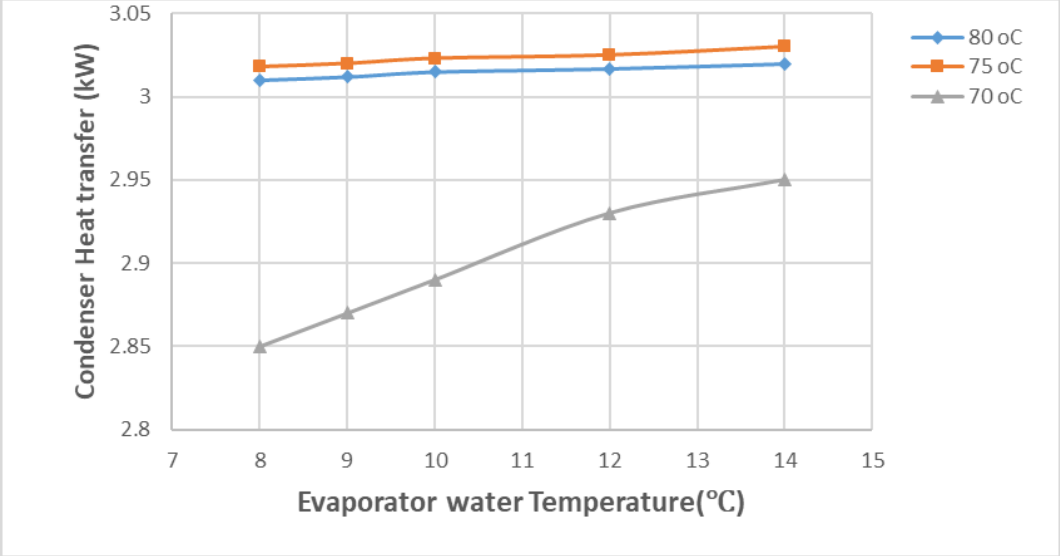

Figure 5: change of condenser rates with tank temperature at 70 kg/hr

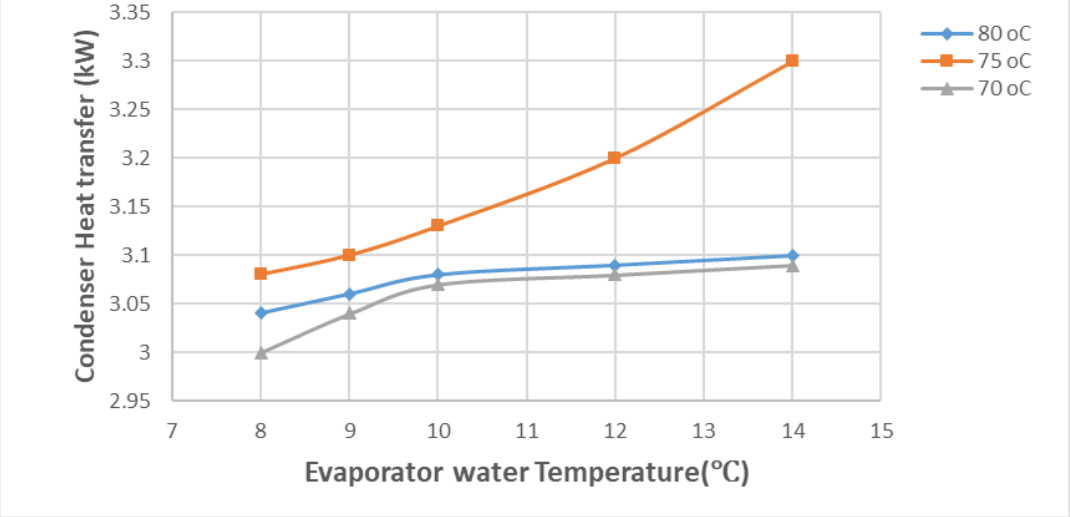

Figure 6: change of condenser rates with tank temperature at kg/hr

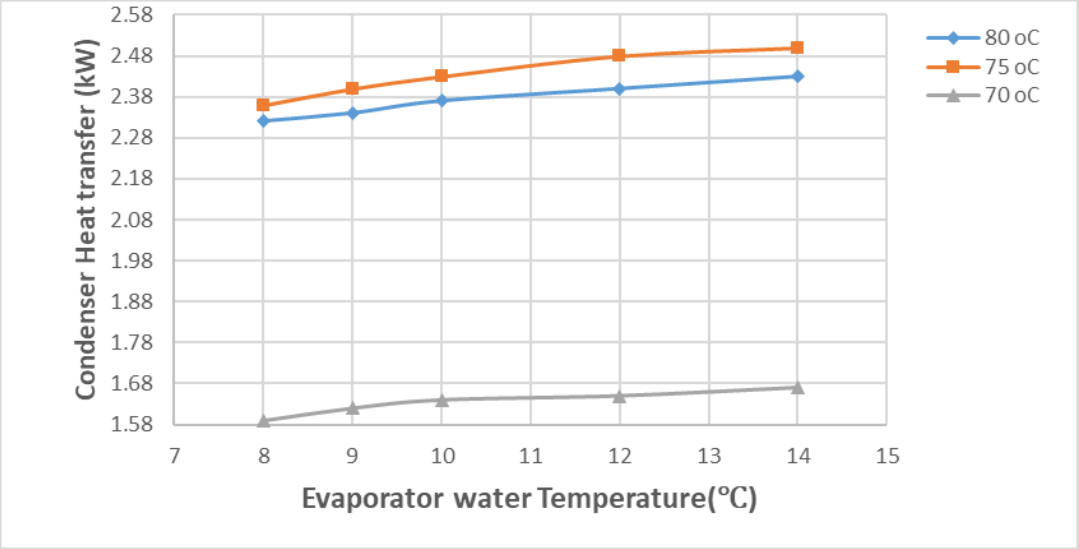

Figure 7: change of condenser rates with tank temperature at 30 kg/hr

3.4 The Effect of Power Consumption and COP

The difference in compressor power consumption with the water temperature and mass flow rate system was investigated in Figures 8,9, and 10. The change in temperature from 8°C to 14°C, while the water flow rate was adjusted to 70, 50, and 30 kg/h [29]. The results reveal a clear dependence of compressor performance on both operating parameters. As the evaporator water temperature increased, the compressor power consumption rose significantly from 650 W to 1050 W. This behavior is credited to the decrease in the cooling consequence at higher evaporator temperatures, which requires the compressor to operate at higher load conditions to maintain the desired cooling capacity [30]. At a fixed flow rate, increasing the evaporator water temperature caused a noticeable increase in suction pressure, thereby raising the compressor discharge pressure and overall energy consumption. Conversely, reducing the water flow rate led to an improvement in the heat exchange process between the solar collector and the evaporator, resulting in a slightly lower compressor load at lower flow rates [31]. Among the tested conditions, the lowest power consumption was observed at 8°C and 30 kg/h, whereas the maximum power consumption occurred at 14°C and 70 kg/h [32].

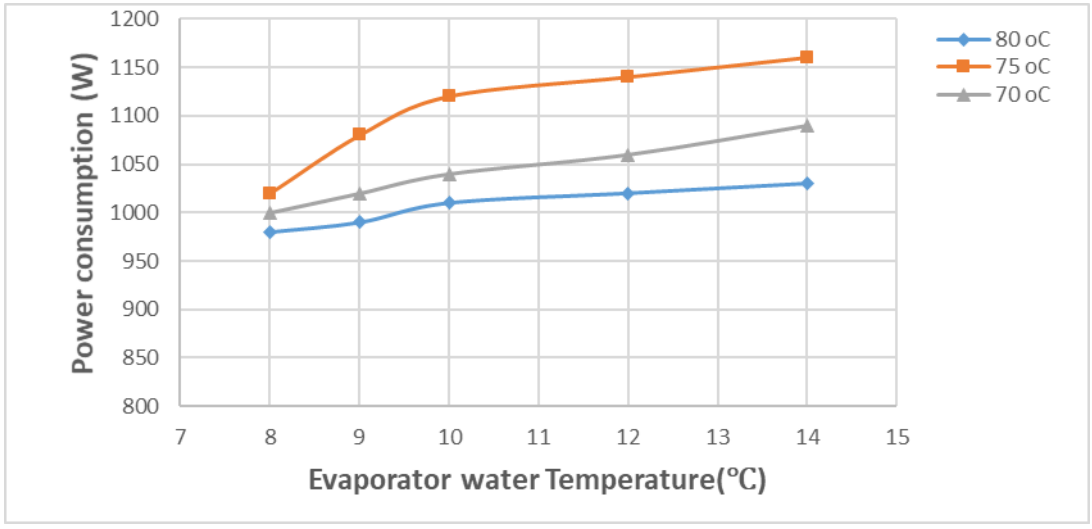

Figure 8: Change of compressor power with Temperature at 70 kg/hr

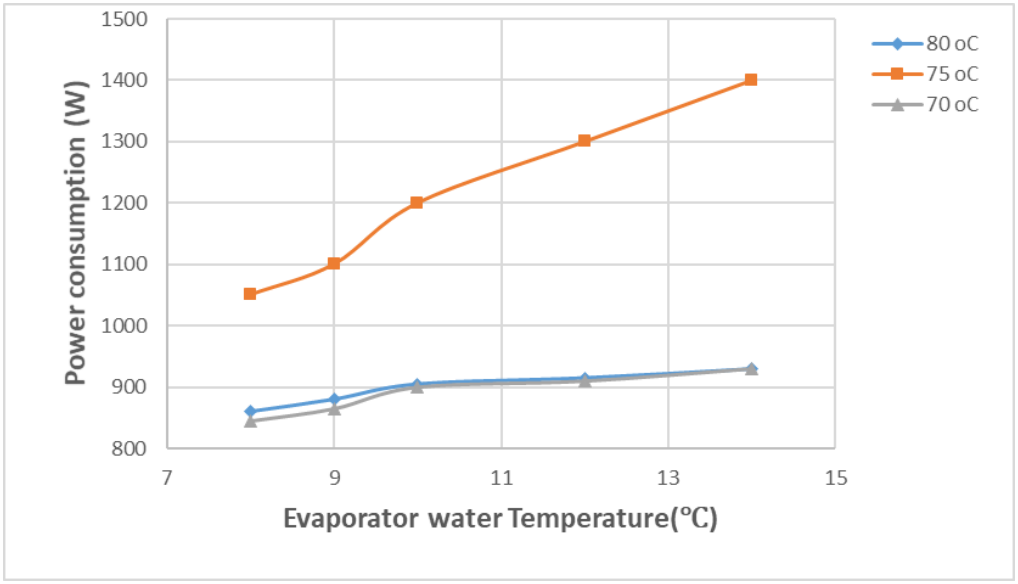

Figure 9: Change of compressor power with Temperature at 50 kg/hr

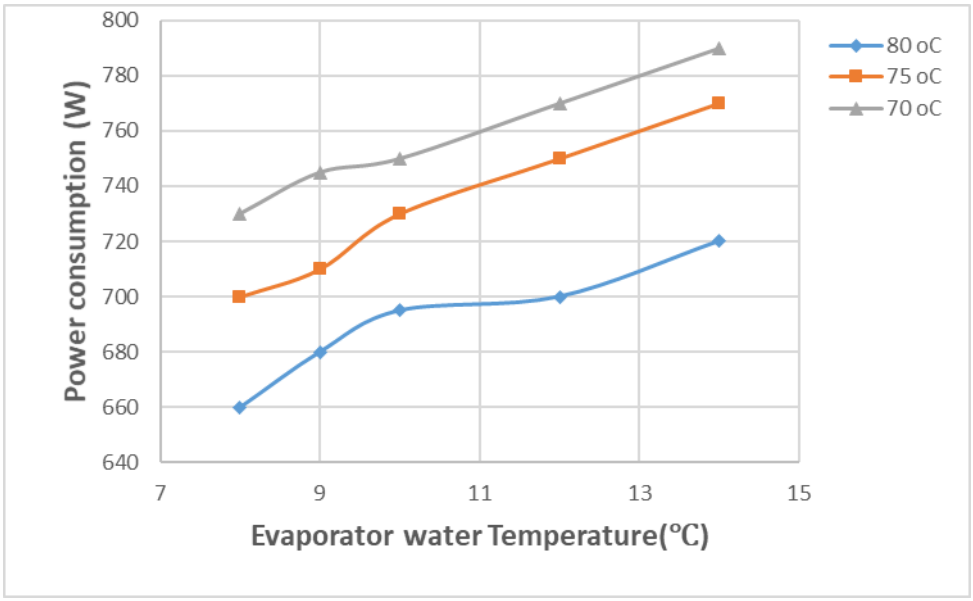

Figure 10: Change of compressor power with Temperature at 30 kg/hr

The effect of cooling water discharge on the compressor power consumption of the hybrid system was examined while maintaining the evaporator water temperature range between 8°C and 14°C. The experimental results indicate that as the cooling water flow rate increased from 30 kg/h to 70 kg/h, as shown in Figures 11,12, and 13 . This increase is mainly attributed to the enhanced heat transfer rate at higher flow rates, which elevates the evaporating pressure and subsequently raises the compressor's discharge pressure and workload [33].

At lower flow rates (30–50 kg/h), the system exhibited relatively stable operation with lower compressor energy consumption, suggesting more favorable thermodynamic conditions for efficient heat absorption from the evaporator [34] . However, at higher flow rates (above 50 kg/h), the compressor demand increased sharply, leading to a reduction in the overall coefficient of presentation. The results emphasize that an optimal cooling flow rate exists, balancing sufficient heat removal from the evaporator with minimal compressor energy input. Hence, operating the system near the moderate flow range provides better energy efficiency and stable cooling performance for solar-assisted air-conditioning applications [35].

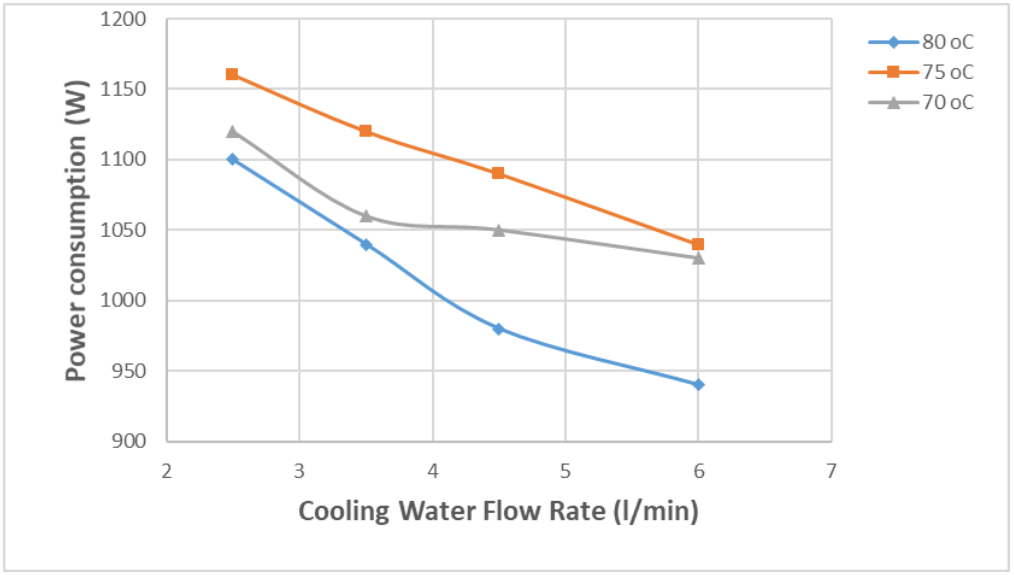

Figure 11: change of compressor power with cooling water discharge at 70 kg/hr

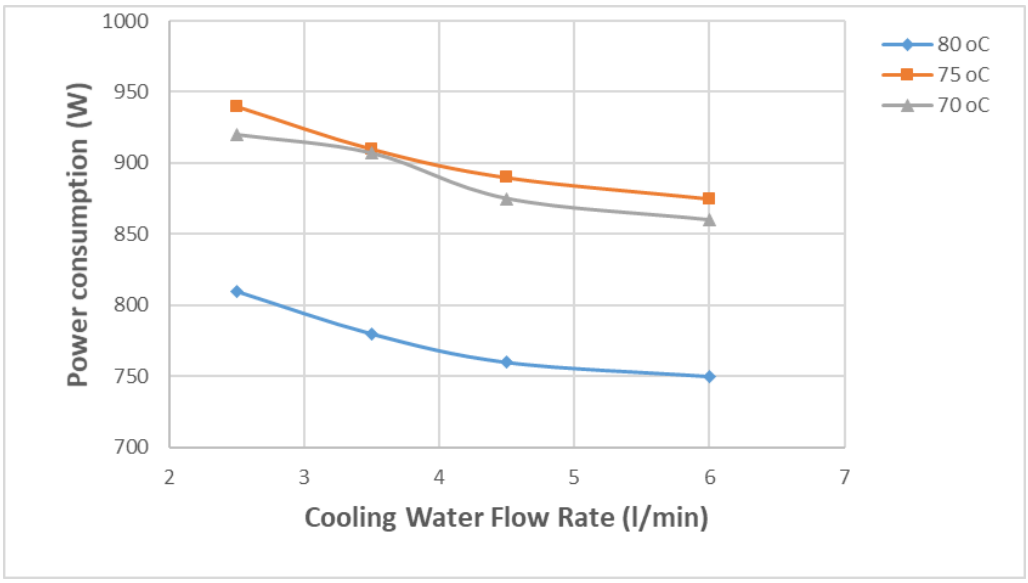

Figure 12: change of compressor power with cooling water discharge at 50 kg/hr

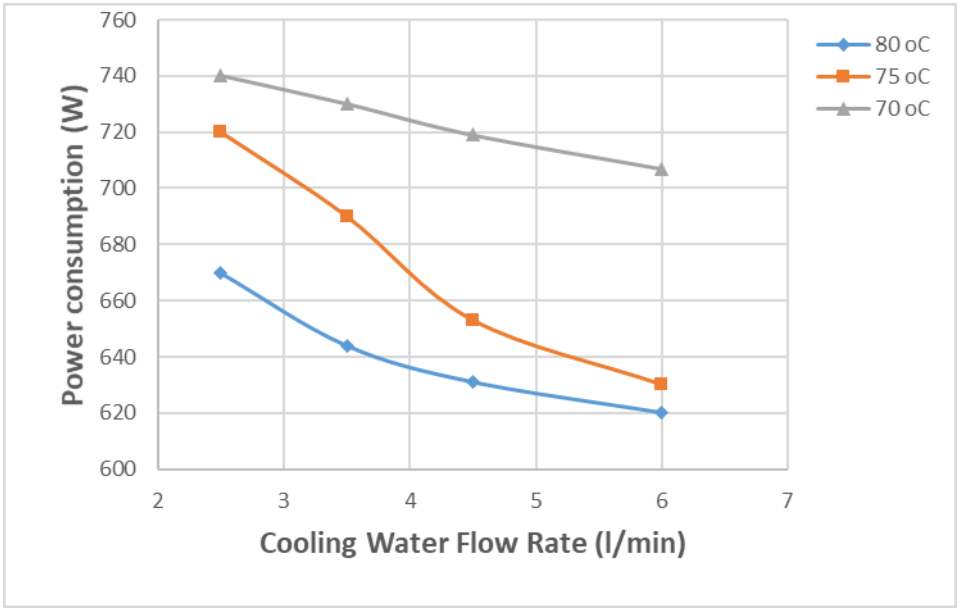

Figure 13: change of compressor power with cooling water discharge at 30 kg/hr

The difference in the coefficient of presentation (COP) with respect to changes in the flow rate was investigated for the hybrid design system. The flow rate was adjusted from 30 kg/h to 70 kg/h, while the evaporator water temperature varied from 8°C to 14°C. The results demonstrate that the COP decreases progressively with increasing cooling water flow rate. At lower flow rates, the system achieved a higher COP due to more effective utilization of the solar thermal input and reduced compressor work. As the flow rate increased, the compressor power demand rose faster than the corresponding increase in cooling capacity, resulting in a net decline in COP as shown in Figures 14,15, and 16 [36].

At the low mass flow rate of 30 kg/h, the system reached its all-out COP, indicating that the refrigerant and evaporator water had sufficient time for efficient heat exchange. However, as the flow rate increased to 50 kg/h and 70 kg/h, the COP values declined because the higher water velocity reduced the temperature difference across the heat exchanger, thereby lowering the overall thermal effectiveness.

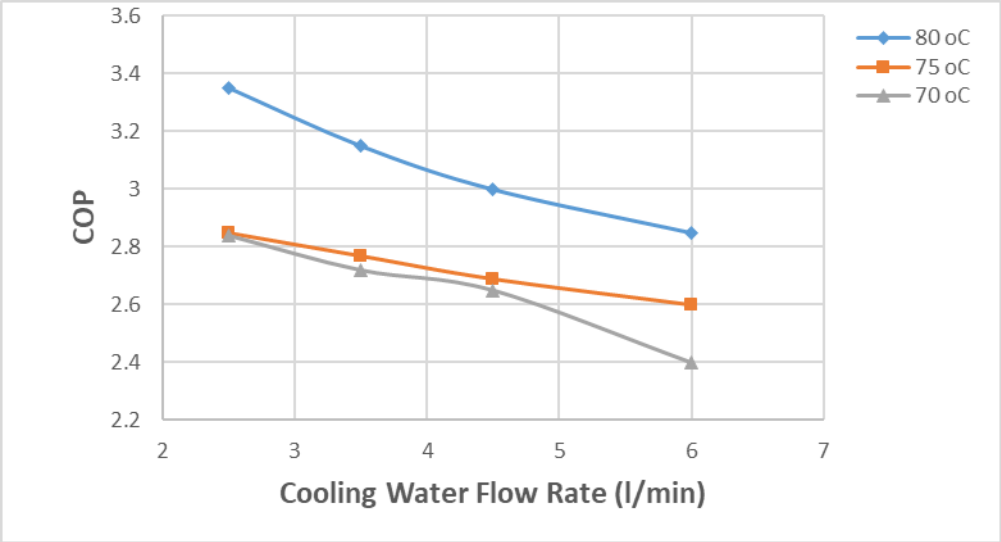

Figure 14: change of COP with cooling discharge rate at 70 kg/hr

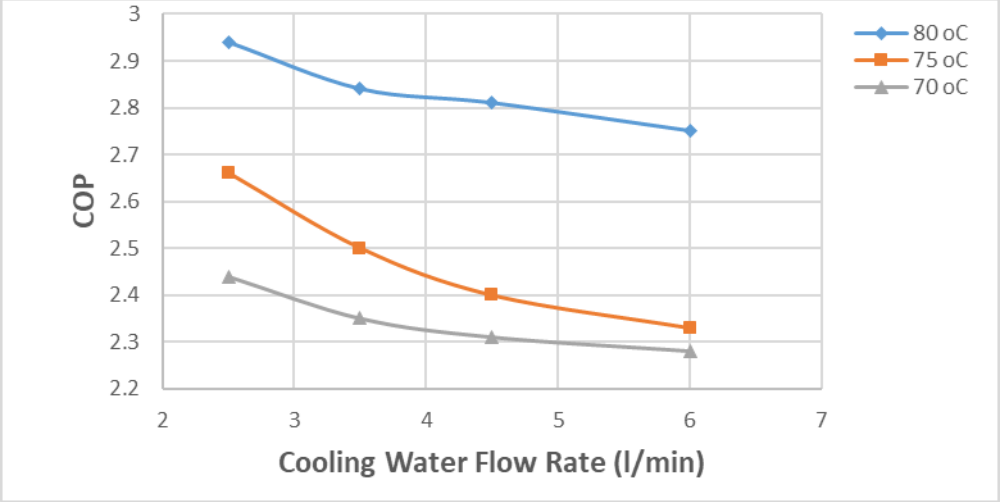

Figure 15: change of COP with cooling discharge rate at 50 kg/hr

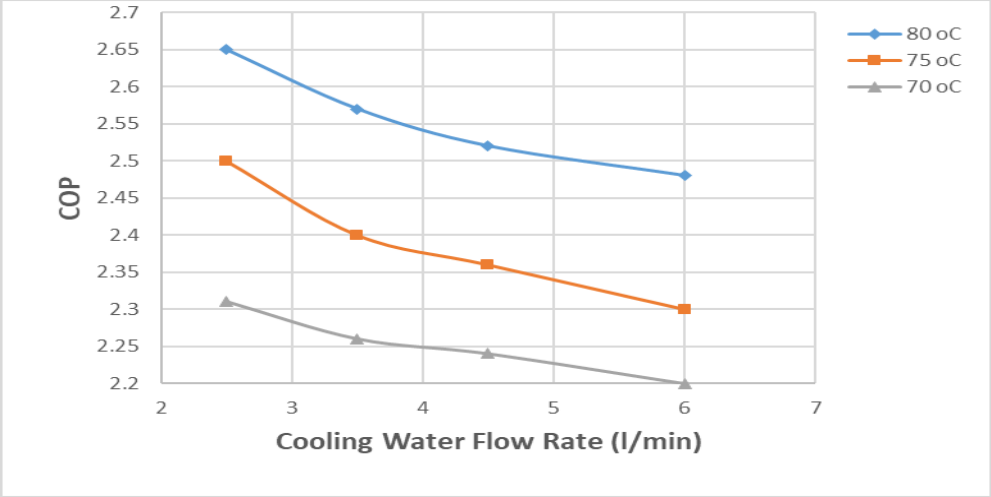

Figure 16: change of COP with cooling discharge rate at 30 kg/hr

7. Conclusions

In conclusion, the hybrid of renewable energy sources into air conditioning designs signifies a transformative step to attaining energy efficiency, conservation, sustainability, and reduced reliance on fossil fuels. A detailed debate is given on the growth and process characteristics of solar thermal energy-powered air conditioning and cooling design. The system's thermal presentation is meaningfully wedged by the temperature of the evaporator water (load). A higher load temperature increases the evaporation temperature, which increases the average cooling capacity from 1500 W to 2900 W. Moreover, there is an upsurge in compressor power practice. As a consequence of these influences, the COP designs dropped from 2.8 to 2 as the evaporation temperature increased from 8 to 14 °C.

References

1. C. Brahmankar, H. Bhushan, A. Ghule, and H. Ranjan, “Study of solar-thermal collector assisted hybrid split air conditioner,” *Int. Res. J. Eng. Technol.*, vol. 5, no. 4, pp. 2921–2925, 2018, [Online]. Available: www.irjet.net
2. R. Gugulothu, N. S. Somanchi, H. B. Banoth, and K. Banothu, “A Review on Solar Powered Air Conditioning System,” *Procedia Earth Planet. Sci.*, vol. 11, pp. 361–367, 2015, doi: 10.1016/j.proeps.2015.06.073.
3. R. Simonetti, L. Molinaroli, and G. Manzolini, “Experimental performance evaluation of a solar-assisted heat pump driven by PV/T panels in real ambient conditions,” *Proc. ISES Sol. World Congr. 2019 IEA SHC Int. Conf. Sol. Heat. Cool. Build. Ind. 2019*, pp. 213–223, 2020, doi: 10.18086/swc.2019.05.07.
4. Z. Wang, M. Luther, P. Horan, J. Matthews, and C. Liu, “Residential space heating electrification through a PV-driven hot water heat pump,” *Energy Build.*, vol. 330, p. 115319, 2025.
5. A. Le Donne, A. Scaccabarozzi, S. Tombolato, S. Binetti, M. Acciarri, and A. Abbotto, “Solar Photovoltaics: A Review,” *Rev. Adv. Sci. Eng.*, vol. 2, no. 3, pp. 170–178, 2013, doi: 10.1166/rase.2013.1030.
6. S. Hussain, A. Kalendar, M. Z. Rafique, and P. Oosthuizen, “Numerical investigations of solar-assisted hybrid desiccant evaporative cooling system for hot and humid climate,” *Adv. Mech. Eng.*, vol. 12, no. 6, pp. 1–16, 2020, doi: 10.1177/1687814020934999.
7. N. I. Ibrahim, F. A. Al-Sulaiman, S. Rehman, A. Saat, and F. N. Ani, “Economic analysis of a novel solar-assisted air conditioning system with integral absorption energy storage,” *J. Clean. Prod.*, vol. 291, p. 125918, 2021.

8. M. Abdelgaied, M. A. Saber, M. M. Bassuoni, and A. M. Khaira, "Performance improvement of solar-assisted air-conditioning systems by using an innovative configuration of a desiccant dehumidifier and thermal recovery unit," *J. Therm. Anal. Calorim.*, vol. 148, no. 14, pp. 7003–7018, 2023.
9. G. Q. Chaudhary *et al.*, "Transient analysis of an efficient solar assisted air-conditioning system for subtropical climate with various solar thermal collectors," *Energy Convers. Manag. X*, vol. 23, p. 100634, 2024.
10. A. Rahman, N. Abas, S. Dilshad, and M. Shoaib, "Case Studies in Thermal Engineering A case study of thermal analysis of a solar assisted absorption air-conditioning system using R-410A for domestic applications," *Case Stud. Therm. Eng.*, vol. 26, no. December 2020, p. 101008, 2021, doi: 10.1016/j.csite.2021.101008.
11. K. Saka and M. F. Orhan, "Performance assessment and useful solar radiation analysis of a grid-connected photovoltaic plant in Türkiye," *Case Stud. Therm. Eng.*, vol. 73, p. 106565, 2025.
12. F. Zelli, "Groundhog Day at the 2024 United Nations biodiversity conference: What COP 16 can teach us for reforming environmental summits," *Earth Syst. Gov.*, vol. 25, p. 100259, 2025.
13. L. Yang, J. Jiang, T. Liu, Y. Li, Y. Zhou, and X. Gao, "Projections of future changes in solar radiation in China based on CMIP5 climate models," *Glob. Energy Interconnect.*, vol. 1, no. 4, pp. 452–459, 2018.
14. M. A. Al-Obaidi, J. M. Rajab, and A. M. Al-Salihi, "Estimation Global Solar Radiation from Common Meteorological Data Using a Stepwise Multiple Regression Model in Abu Gharib, Iraq," in *IOP Conference Series: Earth and Environmental Science*, IOP Publishing, 2025, p. 12006.
15. M. A. Ali, A. Elsayed, I. Elkabani, M. E. Youssef, and G. E. Hassan, "Evaluation and performance comparison of different models for global solar radiation forecasting: a case study on five cities," *Environ. Dev. Sustain.*, vol. 27, no. 5, pp. 10159–10201, 2025.
16. F. Shahrabi Moghadam, "United Nations Convention on Climate Change and Conference of Parties (COP)," *Sci. J. Ecosph.*, vol. 7, no. 4, pp. 52–55, 2025.
17. J. Bronsther and Y. Xu, "The social costs of solar radiation management," *npj Clim. Action*, vol. 4, no. 1, p. 69, 2025.
18. M. Mahendru, J. S. Parihar, A. Jain, and G. D. Sharma, "The Equity Imperative: Revisiting COP Frameworks Through a Justice Lens," *J. Environ. Assess. Policy Manag.*, vol. 27, no. 04, p. 2550012, 2025.
19. A. El Alfy, D. El-Bassiouny, and L. Cochrane, "Shifting geopolitical sands: COP 28 and the new BRICS+," *Manag. Sustain. An Arab Rev.*, vol. 3, no. 2, pp. 197–206, 2024.
20. S. Akhtar, S. Shaima, G. Rita, A. Rashid, and A. J. Rashed, "Navigating the Global Environmental Agenda: A Comprehensive Analysis of COP Conferences, with a Spotlight on COP28 and Key Environmental Challenges.," *Nat. Environ. Pollut. Technol.*, vol. 23, no. 3, 2024.
21. M. R. Rezvi, F. Shahriar, and Z. Islam, "COP-28 & South Asian countries: Policy challenges and policy options," *Sustain. Clim. Chang.*, vol. 17, no. 4, pp. 231–244, 2024.
22. M. Cabral and M. Dillender, "The impact of benefit generosity on workers' compensation claims: Evidence and implications," *Am. Econ. J. Appl. Econ.*, vol. 16, no. 3, pp. 436–481, 2024.
23. J. R. Serrano, L. M. García-Cuevas, A. Gómez-Vilanova, and J. A. López-Carrillo,

"Experimental COP optimization procedure in an air-based reverse Brayton cycle for cryogenic applications," *Appl. Therm. Eng.*, vol. 255, p. 123946, 2024.

24. D. Bogdanov, R. Satymov, and C. Breyer, "Impact of temperature dependent coefficient of performance of heat pumps on heating systems in national and regional energy systems modelling," *Appl. Energy*, vol. 371, p. 123647, 2024.
25. X. Tan, J. Long, J. Li, Z. Li, H. Jiang, and H. Liu, "Dynamic characteristics of refrigerant evaporation temperature in air-water heat source heat pump," *Appl. Therm. Eng.*, vol. 247, p. 123128, 2024.
26. C. E. Rojas-Sánchez and R. A. Hernández-Chaverri, "Effect of temperature on water evaporation coefficient (E) in a thermobalance: A solar-driven steam generation approach," *Energy*, vol. 2, no. 3, p. 188, 2024.
27. S. A. Reda, "Numerical analysis of evaporation process in the heating column of a solar water desalination plant under various geometries, ambient conditions, solar radiations, and time steps," *Results Eng.*, vol. 23, p. 102775, 2024.
28. S. Maleki, S. H. Mohajeri, M. Mehraein, and A. Sharafati, "Lake evaporation in arid zones: Leveraging Landsat 8's water temperature retrieval and key meteorological drivers," *J. Environ. Manage.*, vol. 355, p. 120450, 2024.
29. W. Amin, S. Xie, L. Vasa, and U. Mentel, "Role of land use, green energy, and water resources for food accessibility: Evidence from emerging economies in the lens of COP 28," *L. Degrad. Dev.*, vol. 35, no. 15, pp. 4607–4622, 2024.
30. R. Leal-Arcas, "Global Energy Transition: Reflecting on COP 28 and Case Studies of Qatar and Morocco," *Forthcom. Florida J. Int. Law*, vol. 35, no. 1, 2024.
31. P. Aranguren *et al.*, "Effect of thermoelectric subcooling on COP and energy consumption of a propane heat pump," *Appl. Therm. Eng.*, vol. 257, p. 124242, 2024.
32. A. E. M. Elnaggar, S. Sharaf, Z. S. Abedel Rehim, M. A. El-Bayoumi, H. M. M. Mustafa, and H. M. El Zoghby, "Enhancing COP and cooling temperature for Peltier with decreasing power, and chemical composition negative effect by optimizing connection, position angle, and voltages," *Egypt. J. Chem.*, vol. 67, no. 13, pp. 453–459, 2024.
33. Z. Jia, M. Alharthi, T. Haijun, S. Mehmood, and I. Hanif, "Relationship between natural resources, economic growth, and carbon emissions: the role of fintech, information technology and corruption to achieve the targets of COP-27," *Resour. Policy*, vol. 90, p. 104751, 2024.
34. D. Sun and Z. Liu, "Performance and economic study of a novel high-efficiency PEMFC vehicle thermal management system applied for cold conditions," *Energy*, vol. 305, p. 132415, 2024.
35. J. Ko and J. H. Jeong, "Effects of capillary tube clogging on the energy consumption of a household refrigerator-freezer with a dual evaporation circuit," *Appl. Therm. Eng.*, vol. 238, p. 122219, 2024.
36. K. N. Çerçi, I. R. O. Silva, and K. Hooman, "Investigation of the energetic and exergetic performance of hybrid rotary desiccant-vapor compression cooling systems using different refrigerants," *Energy*, vol. 302, p. 131732, 2024.